Site-Directed Sulfhydryl Labeling of the Lactose Permease of *Escherichia coli*: Helix X†

Pushpa Venkatesan,‡ Yonglin Hu, and H. Ronald Kaback*

Howard Hughes Medical Institute, Departments of Physiology and Microbiology & Molecular Genetics, Molecular Biology Institute, University of California—Los Angeles, Los Angeles, California 90095-1662

Received February 25, 2000; Revised Manuscript Received June 2, 2000

ABSTRACT: Helix X in the lactose permease of *Escherichia coli* contains two residues that are irreplaceable with respect to active transport, His322 and Glu325, as well as Lys319, which is charge-paired with Asp240 in helix VII. Structural and dynamic features of transmembrane helix X are investigated here by site-directed thiol modification of 14 single-Cys replacement mutants with *N*-[^{14}C]ethylmaleimide (NEM) in right-side-out membrane vesicles. Permease mutants with a Cys residue at position 326, 327, 329, 330, or 331 in the cytoplasmic half of the transmembrane domain are alkylated by NEM at 25 °C, a mutant with Cys at position 315 at the periplasmic surface is labeled in the presence of substrate exclusively, and mutants with Cys at positions 317, 318, 320, 321, 324, 328, 332, or 333 do not react with NEM under the conditions tested. Binding of substrate causes increased labeling of a Cys residue at position 315 and decreased labeling of Cys residues at positions 326, 327, and 329. Studies with methanethiosulfonate ethylsulfonate indicate that Cys residues at positions 326, 329, 330, and 331 in the cytoplasmic half are accessible to the aqueous phase from the periplasmic face of the membrane. Ligand binding results in clear attenuation of solvent accessibility of Cys at position 326 and a marginal increase in accessibility of Cys at position 327 to solvent. The findings indicate that the cytoplasmic half of helix X is more reactive/accessible to thiol reagents and more exposed to solvent than the periplasmic half. Furthermore, positions that reflect ligand-induced conformational changes are located on the same face of helix X as Lys319, His322, and Glu325.

Many observations demonstrate that helix X in the lactose permease (lac permease)[1] of *Escherichia coli* plays a central role in active transport. (i) Cys-scanning mutagenesis reveals that in addition to residues His322 and Glu325, which play irreplaceable roles in H^+ translocation and coupling (reviewed in refs *1*, *2*), as well as Lys319, which is charge-paired with Asp240 (helix VII) (*3*−*6*), transmembrane domain X contains six positions where Cys substitution followed by treatment with *N*-ethylmaleimide (NEM) leads to low transport activity (*7*). With the exception of position 331, NEM-sensitive positions 315, 323, 326, 329, and 330 occupy the same face of helix X as His322, Glu325, and Lys319, suggesting that this face is important for activity. (ii) Insertion of two or six contiguous His residues between positions 313 and 314 in the periplasmic loop between helices IX and X (loop IX/X) severely compromises activity (*8*). (iii) Helix X is close to helices VIII and IX, which contain two additional irreplaceable residues, Glu269 and Arg302, respectively, as well as helices VII and XI (reviewed in ref *2*). Of particular relevance to the transport mechanism is the proximity between His322 and Glu325 in helix X and Glu269 and Arg302 in helices VIII and IX, respectively. (iv) Mutation of Glu126 (helix IV) or Arg144 (helix V), both of which are critical for substrate binding, causes a conformational change in helix X (*9*). (v) Substrate binding or imposition of a H^+ electrochemical gradient ($\Delta\bar{\mu}_H+$) alters the reactivity of single-Cys V315C or V331C permease toward thiol reagents (*7*, *10*−*12*). (vi) Fluorescence quenching studies using 7,8-dibromododecyl β,D-maltopyranoside with permease mutants containing single-Trp residues or fluorophore-labeled single-Cys residues in helix X imply that the face of the helix with Glu325 becomes more buried in a nonpolar lipid environment when substrate is bound (*13*).

Site-directed sulfhydryl labeling in situ with NEM is useful for delineating ligand-induced conformational changes and solvent accessibility of engineered Cys residues in the permease (*12*, *14*, *15*; preceding papers in this issue). This paper documents structural and dynamic features of transmembrane domain X by using NEM labeling of single-Cys replacement mutants in situ. The results indicate that binding of substrate produces conformational alterations reflected at the periplasmic end and the cytoplasmic half of helix X. In addition, positions that are accessible to the aqueous phase from the periplasmic side of the membrane and/or undergo

† This work was supported in part by NIH Grant DK51131 to H.R.K.

* To whom correspondence should be addressed at HHMI/UCLA, 5-748 MacDonald Research Laboratories, Box 951662, Los Angeles, CA 90095-1662. Telephone: (310) 206-5053. Telefax: (310) 206-8623. E-mail: RonaldK@HHMI.UCLA.edu.

‡ P.V. is the recipient of NIH NRSA Postdoctoral Fellowship 5 F32 DK09287.

[1] Abbreviations: lac permease, lactose permease; Cys-less permease, functional lac permease devoid of Cys residues; TDG, β,D-galactopyranosyl 1-thio-β,D-galactopyranoside; NEM, *N*-ethylmaleimide; MTSES, methanethiosulfonate ethylsulfonate; $\Delta\mu_H+$, H^+ electrochemical gradient across the membrane; IPTG, isopropyl 1-thio-β,D-galactopyranoside; RSO, right-side-out; DTT, dithiothreitol; KP_i, potassium phosphate; NaDodSO4, sodium dodecyl sulfate.

10.1021/bi0004403 CCC: $19.00
Published on Web 08/08/2000

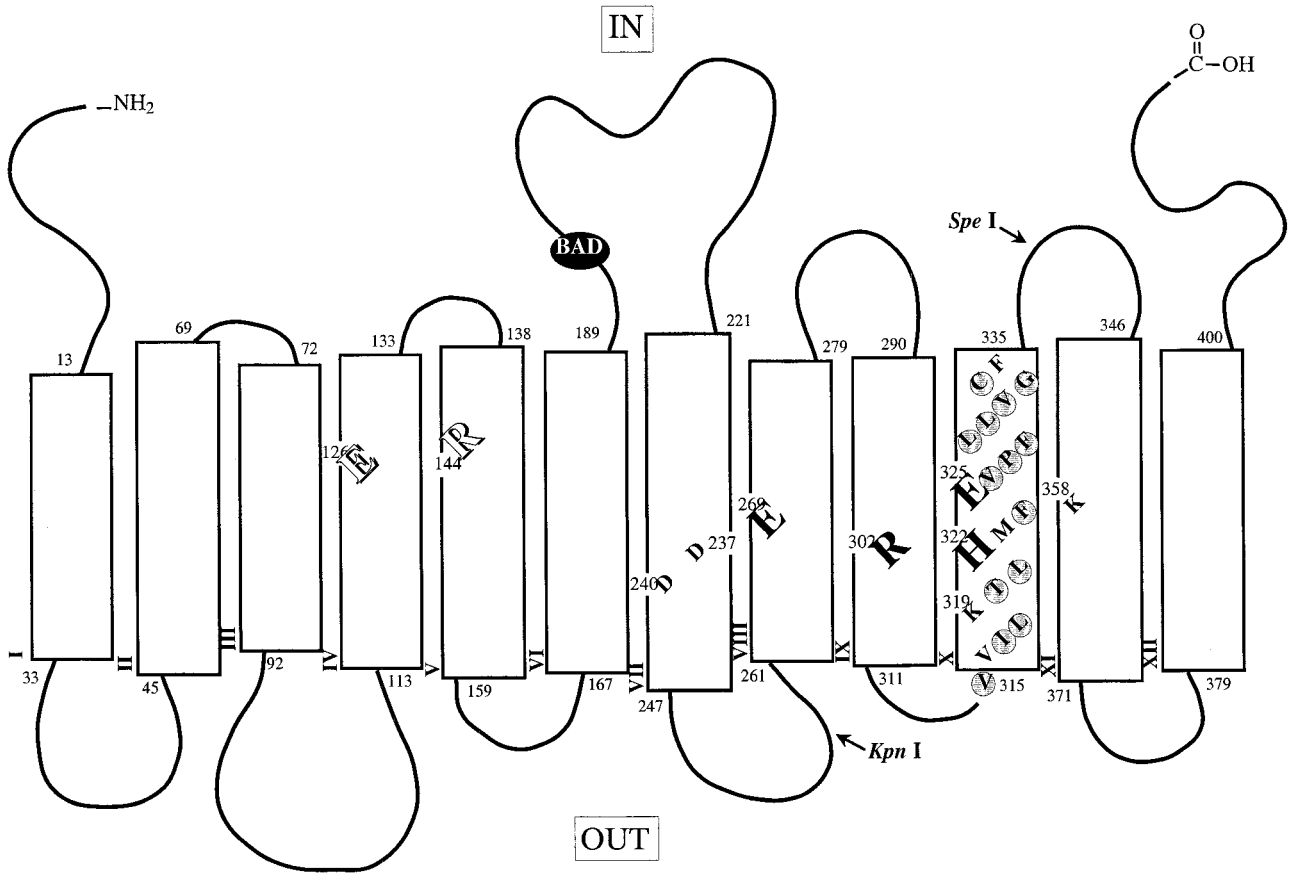

FIGURE 1: Secondary structure model of lac permease. The single-letter amino acid code is used, and putative transmembrane helices are shown in boxes. The six irreplaceable residues Glu126 (helix IV), Arg144 (helix V), Glu269 (helix VIII), Arg302 (helix IX), His322 (helix X), and Glu325 (helix X) are shown as enlarged Roman letters. In addition, the charge pairs Asp237 (helix VII)/Lys358 (helix XI) and Asp240 (helix VII)/Lys319 (helix X) are shown. Residues in helix X studied by site-directed NEM labeling are shown in shaded circles, and the site of the biotin acceptor domain (BAD) is indicated.

a change in solvent accessibility in the presence of ligand are located in the cytoplasmic half of the helix.

EXPERIMENTAL PROCEDURES

Materials. Materials were obtained from sources described previously (Venkatesan, P., Kwaw, I., Hu, Y., and Kaback, H. R., preceding paper in this issue).

Plasmid Construction. Construction of permease mutants containing single-Cys replacements at positions 315, 317, 318, 320, 321, 324, 326, 327, 328, 329, 330, 331, 332, and 333 in a Cys-less background has been described (*7*). To facilitate avidin affinity purification, the DNA fragment encoding a given single-Cys mutant was inserted by restriction fragment replacement into plasmid pKR35/Cys-less *lacY*-L6XB, encoding Cys-less permease with a biotin-acceptor domain in cytoplasmic loop VI/VII (*16*, *17*), using the *Kpn*I and *Spe*I restriction sites. Mutations and insertions were verified by sequencing double-stranded plasmid DNA using the dideoxynucleotide termination method (*18*).

Growth of Bacteria. E. coli T184 (*lacY*$^-$*Z*$^-$) transformed with a plasmid encoding a given mutant was grown as described (Venkatesan, P., Kwaw, I., Hu, Y., and Kaback, H. R., preceding paper in this issue).

Membrane Preparation. Right-side-out (RSO) membrane vesicles were prepared as described (Venkatesan, P., Kwaw, I., Hu, Y., and Kaback, H. R., preceding paper in this issue).

NEM Labeling. Alkylation with [^{14}C]NEM and quantification were performed as described (Venkatesan, P., Kwaw, I., Hu, Y., and Kaback, H. R., preceding paper in this issue).

Labeling with NEM in the Presence of $\Delta\bar{\mu}_H+$. [^{14}C]NEM labeling in the presence of ascorbate and phenazine methosulfate was carried out with given single-Cys mutants as described (Venkatesan, P., Liu, Z., Hu, Y., and Kaback, H. R., preceding paper in this issue).

MTSES Labeling. The reactivity of RSO membrane vesicles containing permease with given single-Cys residues with MTSES was determined as described (Venkatesan, P., Kwaw, I., Hu, Y., and Kaback, H. R., preceding paper in this issue).

Western Blot Analysis. Fractions containing affinity-purified biotinylated permease were analyzed electrophoretically on sodium dodecyl sulfate ($NaDodSO_4$)/12% polyacrylamide gels, and proteins were electroblotted and quantified as described (Venkatesan, P., Kwaw, I., Hu, Y., and Kaback, H. R., preceding paper in this issue).

Protein Determinations. Protein was assayed using a Micro BCA protein determination kit (Pierce Inc., Rockford, IL).

RESULTS

Single-Cys permease mutants containing a Cys residue in place of Val315, Ile317, Leu318, Thr320, Leu321, Phe324, Val326, Pro327C, Phe328, Leu329, Leu330, Val331, Gly332, or containing a single native Cys residue at position 333

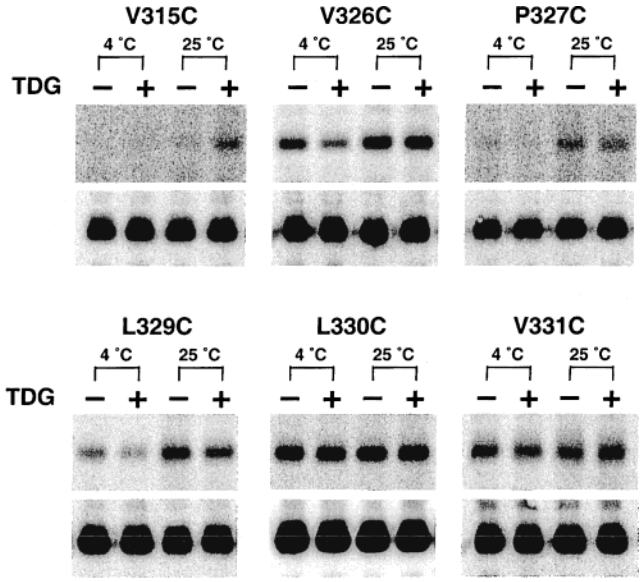

FIGURE 2: Effect of TDG and temperature on NEM labeling of given single-Cys mutants in RSO membrane vesicles. RSO membrane vesicles [0.4 mg of protein in 50 μL of 100 mM KP_i (pH 7.5)/10 mM $MgSO_4$] prepared from *E. coli* T184 transformed with a plasmid encoding an indicated single-Cys mutant were incubated with [^{14}C]NEM (40 mCi/mmol; 0.4 mM final concentration) for 10 min in the absence or presence of 10 mM TDG at 4 or 25 °C as shown. Reactions were terminated with DTT (15 mM final concentration), and biotinylated permease was solubilized and purified by avidin-affinity chromatography as described in Experimental Procedures. Aliquots containing approximately 5 μg of protein were separated by $NaDodSO_4$/12% PAGE, and the labeled protein was visualized by autoradiography (upper panels). A fraction of the protein (0.5 μg) eluted from the avidin-Sepharose beads was analyzed by Western blotting with anti-C-terminal antibody to quantify the amount of permease in each sample (lower panels).

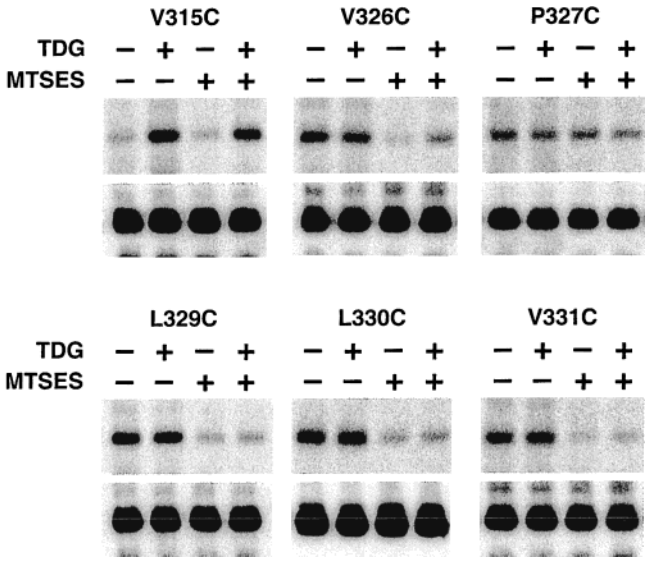

FIGURE 3: Accessibility of given single-Cys permease mutants to MTSES and the effect of TDG. RSO membrane vesicles [0.5−0.6 mg of protein in 0.5 mL of 100 mM KP_i (pH 7.5)/10 mM $MgSO_4$] prepared from *E. coli* T184 transformed with plasmid encoding the indicated single-Cys mutant were incubated without or with MTSES (200 μM final concentration) for 5 min at 25 °C in the absence or presence of TDG, as indicated. Vesicles were washed twice with ice-cold buffer and resuspended in 50 μL of the same buffer, and TDG (10 mM final concentration) was added back to the samples initially treated with TDG. Samples were then treated with [^{14}C]NEM (40 mCi/mmol; 0.4 mM final concentration) for 30 min at 25 °C. Reactions were quenched with DTT, and biotinylated permease was solubilized and purified as described in Experimental Procedures. Aliquots containing approximately 5 μg of protein were separated by $NaDodSO_4$/12% PAGE, and the NEM-labeled protein was visualized by autoradiography (upper panels). A fraction of the protein (0.5 μg) eluted from the avidin-Sepharose beads was analyzed by Western blotting with anti-C-terminal antibody to quantify the amount of permease in each sample (lower panels).

retain the ability to catalyze active lactose transport (*7*) and were included in this study (Figure 1). Single-Cys mutants K319C,[2] H322C, E325C, and F334C, which do not catalyze significant lactose accumulation, and mutants V316C and M323C, which are not alkylated by NEM (*14*), were not included.

NEM Labeling at 25 °C. Permease mutant V326C, L330C, or V331C reacts with [^{14}C]NEM in 10 min at 25 °C (Figure 2, lane 3 in the appropriate panel), and labeling is unchanged in the presence of β-D-galactopyranosyl 1-thio-β,D-galactopyranoside (TDG) (Figure 2, compare lanes 3 and 4 in the appropriate panel), which implies that conformational changes induced by ligand binding are not reflected by the Cys at position 326, 330, or 331 or are not apparent at 25 °C. Mutant V315C reacts with NEM only in the presence of TDG (Figure 2, V315C, lanes 3 and 4), which suggests that binding of substrate induces a structural alteration that causes the Cys side chain at position 315 to become reactive/accessible to the reagent. Labeling of P327C permease by NEM is weak relative to mutant V326C or L330C (Figure 2, lane 3 in the appropriate panels) and is slightly attenuated in the presence of TDG (Figure 2, P327C; compare lanes 3 and 4). Mutant L329C is strongly labeled at 25 °C, and ligand binding causes a small reduction in labeling (Figure 2, L329C, lanes 3 and 4). Permease I317C, L318C, T320C, L321C, F324C, F328C, G332C, or C333 is not alkylated by NEM in the absence or presence of TDG (data not shown).

NEM Labeling at 4 °C. To determine whether minimizing thermal protein motion facilitates detection of ligand-induced conformational changes, alkylation was also carried out at 4 °C for 10 min. Labeling of L330C or V331C permease at 4 °C is intense and comparable to that observed at 25 °C (Figure 2, compare lanes 1 and 3 in the appropriate panels). The observations indicate that the Cys side chain at position 330 or 331 is in an environment that is unhindered and electronically favors reaction with NEM and that accessibility to the reagent is independent of protein thermal motion. No substrate-induced change in labeling of L330C or V331C permease is evident at 4 °C (Figure 2, compare lanes 1 and 2 in the appropriate panels). With V315C permease at 4 °C, the dramatic increase in reactivity observed in the presence of TDG at 25 °C is not observed, suggesting that protein thermal motion is required for labeling the Cys side chain at this position even in the presence of ligand (Figure 2, V315C, compare lanes 1 and 2 with lanes 3 and 4). The extent of labeling of V326C permease at 4 °C is slightly lower than that observed at 25 °C (Figure 2, V326C, compare lanes 1 and 3), suggesting that thermal motion of the protein makes a relatively small contribution to the reactivity/accessibility of the -SH moiety at 25 °C. Ligand-

[2] Site-directed mutants are designated by the single-letter amino acid abbreviation for the targeted residue, followed by the sequence position of the residue in the wild-type lac permease, and followed by a second letter indicating the amino acid replacement.

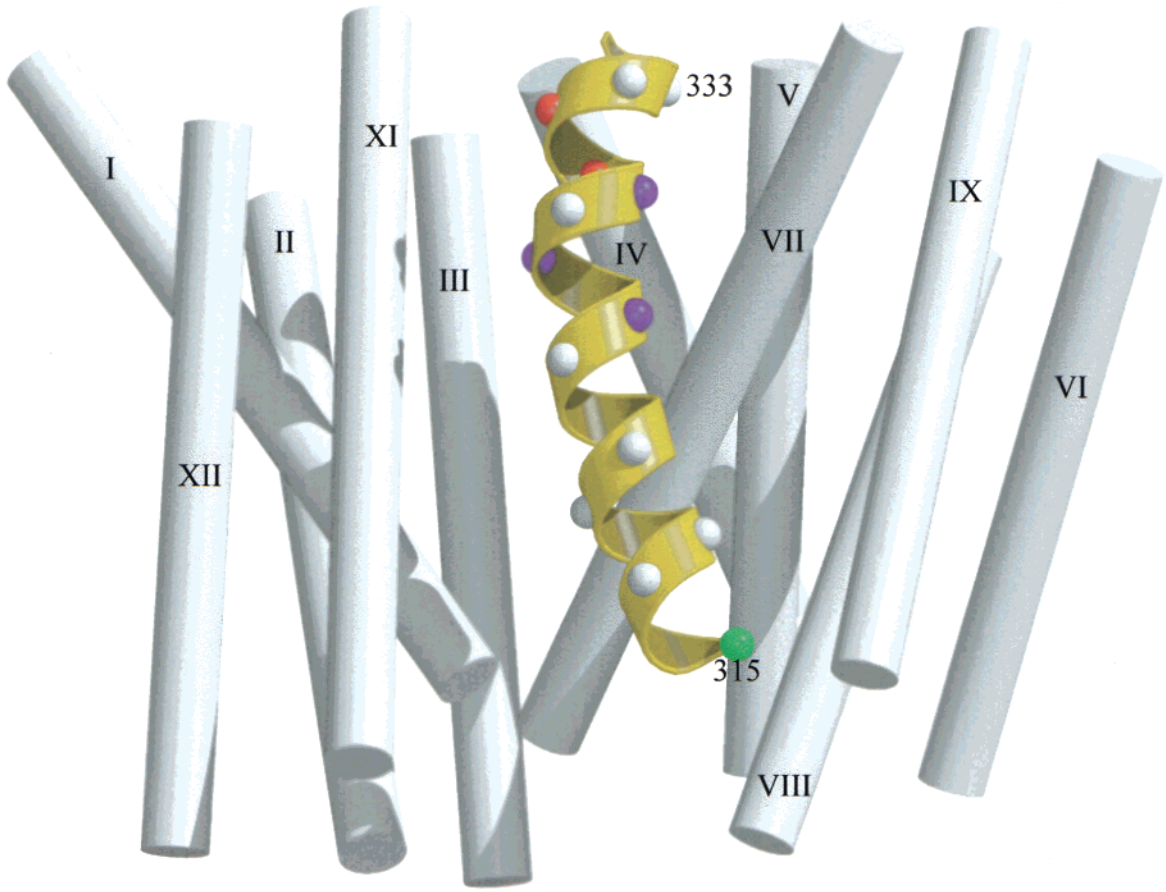

FIGURE 4: NEM labeling and the effect of ligand on single-Cys replacements in helix X. Results from Figure 2 are shown in a 3D representation of helix VII as follows. Positions that label with NEM are presented as colored spheres: red, labels with NEM with no change in the presence of TDG; green, increased labeling in the presence of TDG; and blue, decreased labeling in the presence of TDG. Positions that do not label are shown as white spheres. Helices other than helix VII are shown as rods, and their positions are derived from modeling studies (*27*) using approximately 100 constraints (*2*).

induced conformational changes that are not discernible at 25 °C with V326C permease become apparent at 4 °C where TDG causes a marked decrease in labeling (Figure 2, V326C, compare lanes 1 and 2 with lanes 3 and 4). P327C permease, which is weakly labeled at 25 °C, does not label at 4 °C, implying that protein thermal motion is responsible for labeling at 25 °C (Figure 2, P327C, compare lanes 1 and 2 with lanes 3 and 4). Decreasing the temperature to 4 °C also causes a pronounced decrease in labeling of L329C permease relative to 25 °C (Figure 2, L329C, compare lanes 1 and 3), indicating that thermal motion is largely responsible for intense labeling at 25 °C. However, the extent of substrate-induced attenuation is comparable at both temperatures (Figure 2, compare lanes 1 and 2 with lanes 3 and 4).

Effect of $\Delta\bar{\mu}_H+$ *on Labeling by NEM.* To determine if single-Cys replacement mutants in helix X reflect conformational changes produced by $\Delta\bar{\mu}_H+$, NEM labeling of each mutant was examined in the absence or presence of $\Delta\bar{\mu}_H+$. With the exception of V331C permease, which exhibits a small decrease in labeling in the presence of $\Delta\bar{\mu}_H+$ as reported previously (*12*), labeling of a Cys residue at position 315, 317, 318, 320, 321, 324, 326, 327, 328, 329, 330, 332, or 333 is not significantly altered by $\Delta\bar{\mu}_H+$.

Accessibility to MTSES. Pretreatment of V315C permease with methanethiosulfonate ethylsulfonate (MTSES) (*15*, *19*−*21*) in the absence or presence of TDG has no effect on NEM labeling, indicating that the Cys side chain at position 315 is not accessible to MTSES and therefore not exposed to bulk solvent (Figure 3, V315C, compare lanes 1 and 3 and lanes 2 and 4). NEM labeling of V326C permease is completely blocked by MTSES, showing that this side chain is highly accessible to solvent (Figure 3, V326C, compare lanes 1 and 3). However, when vesicles are treated with MTSES in the presence of TDG, partial restoration of labeling is observed, indicating that position 326 becomes less exposed to solvent when substrate is bound (Figure 3, compare lanes 3 and 4). NEM labeling of P327C permease is unchanged upon prior treatment with MTSES, showing that the Cys side chain is inaccessible to solvent (Figure 3, P327C, compare lanes 1 and 3). However, when treatment with MTSES is carried out in the presence of TDG, slight attenuation of labeling is observed, suggesting that ligand binding partially increases the accessibility of the Cys residue to solvent (Figure 3, compare lanes 2 and 4). Treatment of permease mutants L329C, L330C, or V331C with MTSES in the absence or presence of TDG results in a marked decrease in labeling, showing that the thiol group at these positions is exposed to solvent and that substrate binding does not alter accessibility (Figure 3, compare lanes 1 and 2 with lanes 3 and 4 in the indicated panels).

DISCUSSION

Site-specific alkylation of 14 lac permease mutants containing single-Cys replacements in helix X was initiated

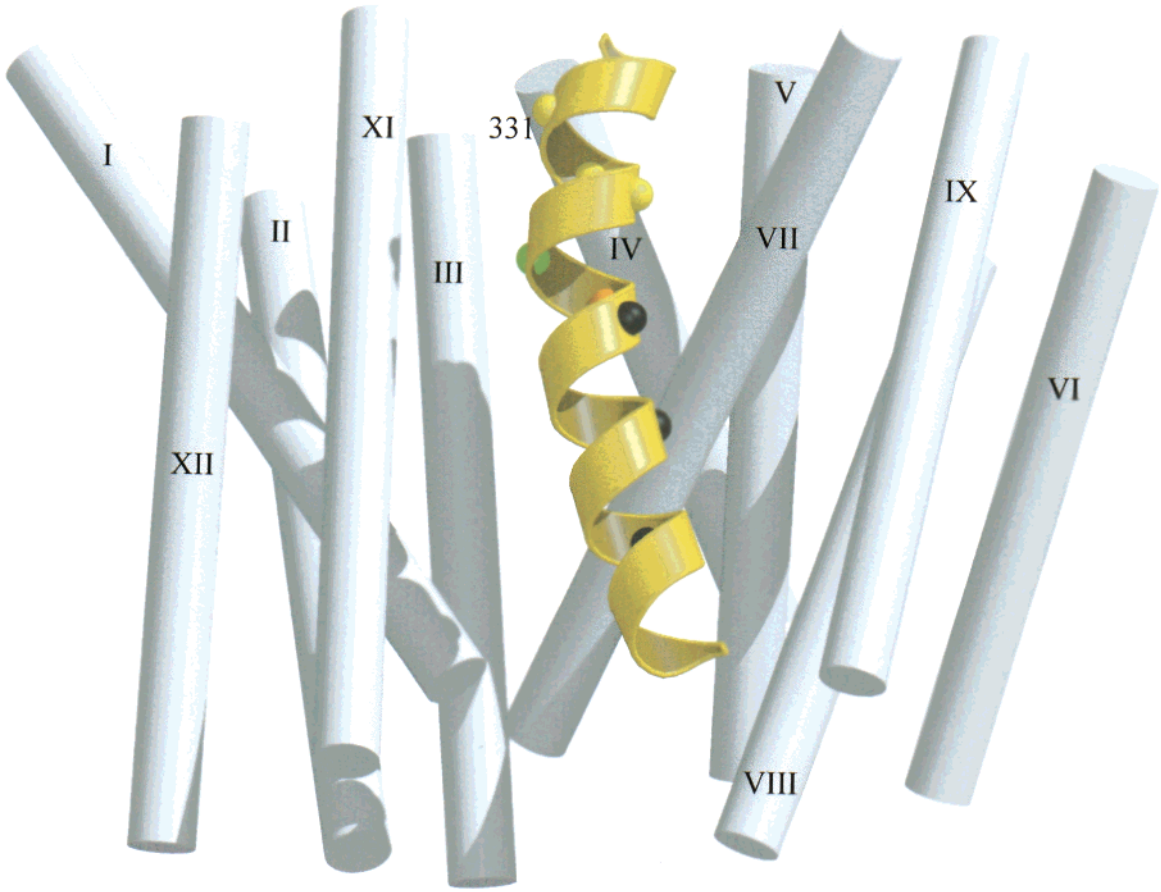

FIGURE 5: Solvent accessibility of single-Cys replacements in helix X as judged by MTSES blockade of NEM labeling. Results from Figure 3 are shown in a 3D representation of helix VII. Positions where NEM labeling is significantly blocked by MTSES are shown as yellow spheres. Position 326 is shown as an orange sphere to indicate decreased accessibility to solvent in the presence of TDG; position 327 is shown as a green sphere to indicate a ligand-induced increase in solvent accessiblity. Helices other than helix VII are shown as rods, and their positions are derived from modeling studies (*27*) using approximately 100 constraints (*2*). Residues Glu325, His322, and Lys319 are shown as black spheres.

to study structural and dynamic features of this mechanistically important transmembrane domain. The cytoplasmic half of helix X clearly labels with NEM more readily than the periplasmic half (Figure 4). Thus, a Cys residue at position 326, 329, 330, or 331 is strongly labeled by NEM, a Cys at position 327 shows weak labeling, and a Cys at position 328, 332, or 333 does not label. In contrast, with the exception of mutant V315C, which labels only in the presence of TDG, none of the Cys substitutions at position 316, 317, 318, 320, 321, 323, or 324 in the periplasmic half of helix X label with NEM. Most of the unreactive Cys replacements lie either at the presumed interface between helix X and the interior of the bilayer or in regions abutting other helices. Tertiary contacts within the protein or between the permease and the lipid bilayer may sterically and/or electronically disfavor alkylation of the thiol group in these mutants. Furthermore, poor labeling of Cys residues in the periplasmic half of helix X is suggestive of tighter tertiary packing between helix X and the neighboring helices in the periplasmic half relative to the cytoplasmic half of helix X.

Ligand-induced conformational changes within the permease are reflected by altered labeling of Cys residues at positions 315, 326, 327, and 329 in the presence of TDG, the most dramatic being V315C permease, which labels only in the presence of ligand (Figure 4). In contrast, Cys residues at positions 326, 329, and 327 undergo attenuation in labeling in the presence of TDG. Thus, substrate binding enhances labeling at the periplasmic end of helix X (position 315) and decreases labeling in the cytoplasmic half of the helix (positions 326, 327, and 329). Similar results have been observed with single-Cys replacement mutants in helix II (Venkatesan, P., Liu, Z., Hu, Y., and Kaback, H. R., preceding paper in this issue), where TDG enhances labeling at positions 45, 49, and 53 in the periplasmic half and decreases labeling at positions 60 and 67 in the cytoplasmic half. In any case, the finding that Cys residues at positions 315, 326, 327, and 329 reflect structural changes upon ligand binding supports the conclusion from Cys-scanning mutagenesis studies (*7*) that the face of helix X with these positions may be important for the conformational alterations that occur during substrate/H^+ symport.

Since transmembrane helix X contains residues that play an essential role in the coupling between H^+ and substrate translocation, the effect of $\Delta\bar{\mu}_H+$ on NEM labeling was also tested. Previous findings (*7*, *10*−*12*) indicate that either imposition of $\Delta\bar{\mu}_H+$ or ligand binding alters the NEM reactivity of V315C or V331C permease. Although V315C permease labels with NEM in the presence of ligand exclusively, only slight attenuation is observed with mutant V331C, and labeling of neither mutant is altered by $\Delta\bar{\mu}_H+$. It is likely that the apparent differences are related to the use of labeling reagents other than NEM and/or different

labeling conditions. Importantly, none of the other Cys replacement mutants within helix X or helix II (Venkatesan, P., Liu, Z., Hu, Y., and Kaback, H. R., preceding paper in this issue) exhibit altered reactivity upon imposition of $\Delta\bar{\mu}_H+$, a finding consistent with the conclusion that ligand binding and dissociation are the primary driving forces for turnover of the permease (*2*).

Thermal motion markedly influences labeling of several Cys residues in helices VII, II (accompanying papers in this issue), and X. Labeling at 4 °C frequently reveals substrate-induced structural alterations at positions that are not observed at 25 °C. A comparison of the extent of labeling at 25 and 4 °C indicates qualitatively the contribution of protein dynamics to the reactivity/accessibility of a given Cys residue. Labeling of V315C permease at 25 °C in the presence of ligand only, as well as the relatively low reactivity of P327C permease at 25 °C and the complete lack of labeling observed with these mutants at 4 °C, implies that protein thermal motion is primarily responsible for the reactivity of Cys residues at these positions. Likewise, thermal motion contributes to the reactivity of permease mutants V326C and L329C, where labeling at 4 °C is lower than observed at 25 °C. Interestingly, with V326C permease, substrate-induced attenuation that is not evident at 25 °C becomes readily apparent at 4 °C. In contrast, the relatively intense labeling of mutants L330C and V331C at high and low temperature suggests that the reactivity/accessibility of the thiol groups at these positions in the cytoplasmic end of helix X is not altered by protein dynamics.

As observed with helix II (Venkatesan, P., Liu, Z., Hu, Y., and Kaback, H. R., preceding paper in this issue), thiol modification studies with the hydrophilic reagent MTSES indicate that the solvent-accessible positions in helix X are also located in the cytoplasmic half of the domain (Figure 5). Remarkably, a Cys residue at position 315 at the periplasmic end of helix X is not accessible to the aqueous phase, while Cys residues at positions 326, 329, 330, and 331 in the cytoplasmic half are accessible. Binding of substrate is accompanied by alterations in the solvent accessibility of specific positions in the cytoplasmic half of helix X. A Cys residue at position 326 undergoes a clear decrease in solvent accessibility in the presence of ligand, while a Cys at position 327 responds in the opposite manner, becoming slightly more exposed to solvent. No such alterations are evident in the periplasmic half of helix X. Since only certain positions or groups of positions within transmembrane domains appear to be exposed to solvent, and substrate binding causes distinct alterations in solvent accessibility, it is likely that the MTSES-reactive positions are part of the solvent-filled cleft in the permease (*22*−*26*) and that this structure may represent at least part of the translocation pathway for sugar and/or H^+.

ACKNOWLEDGMENT

We are deeply indebted to Mark Girvin for molecular modeling. In addition, we thank Kerstin Stempel for help with the preparation of the figures.

REFERENCES

1. Kaback, H. R., and Wu, J. (1997) *Q. Rev. Biophys. 30*, 333−364.
2. Kaback, H. R., and Wu, J. (1999) *Acc. Chem. Res. 32*, 805−813.
3. Sahin-Tóth, M., Dunten, R. L., Gonzalez, A., and Kaback, H. R. (1992) *Proc. Natl. Acad. Sci. U.S.A. 89*, 10547−10551.
4. Sahin-Tóth, M., and Kaback, H. R. (1993) *Biochemistry 32*, 10027−10035.
5. Lee, J. L., Hwang, P. P., Hansen, C., and Wilson, T. H. (1992) *J. Biol. Chem. 267*, 20758−20764.
6. Voss, J., Sun, J., and Kaback, H. R. (1998) *Biochemistry 37*, 8191−8196.
7. Sahin-Tóth, M., and Kaback, H. R. (1993) *Protein Sci. 2*, 1024−1033.
8. McKenna, E., Hardy, D., and Kaback, H. R. (1992) *Proc. Natl. Acad. Sci. U.S.A. 89*, 11954−11958.
9. Venkatesan, P., and Kaback, H. R. (1998) *Proc. Natl. Acad. Sci. U.S.A. 95*, 9802−9807.
10. Jung, H., Jung, K., and Kaback, H. R. (1994) *Protein Sci. 3*, 1052−1057.
11. Wu, J., Frillingos, S., Voss, J., and Kaback, H. R. (1994) *Protein Sci. 3*, 2294−2301.
12. Frillingos, S., and Kaback, H. R. (1996) *Biochemistry 35*, 3950−3956.
13. Wang, Q., Matsushita, K., de Foresta, B., LeMaire, M., and Kaback, H. R. (1997) *Biochemistry 36*, 14120−14127.
14. Frillingos, S., Wu, J., Venkatesan, P., and Kaback, H. R. (1997) *Biochemistry 36*, 6408−6414.
15. Frillingos, S., and Kaback, H. R. (1997) *Protein Sci. 6*, 438−443.
16. Consler, T. G., Persson, B. L., Jung, H., Zen, K. H., Jung, K., Prive, G. G., Verner, G. E., and Kaback, H. R. (1993) *Proc. Natl. Acad. Sci. U.S.A. 90*, 6934−6938.
17. Sun, J., and Kaback, H. R. (1997) *Biochemistry 36*, 11959−11965.
18. Sanger, F., Nicklen, S., and Coulsen, A. R. (1977) *Proc. Natl. Acad. Sci. U.S.A. 74*, 5463−5467.
19. Akabas, M. H., Stauffer, D. A., Xu, M., and Karlin, A. (1992) *Science 258*, 307−310.
20. Stauffer, D. A., and Karlin, A. (1994) *Biochemistry 33*, 6840−6849.
21. Karlin, A., and Akabas, M. H. (1995) *Neuron 15*, 1231−1244.
22. Costello, M. J., Viitanen, P., Carrasco, N., Foster, D. L., and Kaback, H. R. (1984) *J. Biol. Chem. 259*, 15579−15586.
23. Costello, M. J., Escaig, J., Matsushita, K., Viitanen, P. V., Menick, D. R., and Kaback, H. R. (1987) *J. Biol. Chem. 262*, 17072−17082.
24. Li, J., and Tooth, P. (1987) *Biochemistry 26*, 4816−4823.
25. Li, J., and Tooth, P. (1988) *Prog. Clin. Biol. Res. 273*, 93−98.
26. Zhuang, J., Privé, G. G., Verner, G. E., Ringler, P., Kaback, H. R., and Engel, A. (1999) *J. Struct. Biol. 125*, 63−75.
27. Rastogi, V. K., and Girvin, M. E. (1999) *Nature 402*, 263−268.

BI0004403